Small-Scale Indoor Channel Measurements at 24 GHz on a University Campus

Mohammad Abo rahama, Amer Zakaria, Mahmoud H. Ismail, Marawan El-Bardicy and Mohamed El-Tarhuni
Department of Electrical Engineering, American University of Sharjah
PO Box 26666, Sharjah, UAE

***Abstract*—In this paper, small-scale indoor channel measurements at millimeter wave frequencies are conducted at the American University of Sharjah campus in the United Arab Emirates. The measurements are performed using a wideband correlation-based channel sounder, which uses a 250 MHz bandwidth signal modulating a 24 GHz carrier. Different indoor scenarios are considered to examine the effect of the environment on the channel characteristics. The measurements are analyzed to obtain the channel's power delay profile, from which various parameters are calculated such as the average excess delay, the delay spread, and the number of resolvable multipath components.**

***Index Terms*—Channel models, Millimeter wave propagation, 5G mobile communication.**

I. Introduction

For the past year, more and more operators have been deploying fifth generation new radio (5G-NR) cellular networks in cities worldwide. The demand for next generation cellular systems stems from the need for more bandwidth as more devices need to be connected [1], [2]. With 5G-NR systems, more bandwidth will be available as higher millimeter wave (mm-Wave) carrier frequencies are being considered; these frequencies range from 24.5 GHz to 52.6 GHz [3].

The proper deployment of wireless systems using mm-Waves necessitates accurate channel modeling to allow for coverage prediction and performance evaluation of these systems. This motivated several research groups to conduct large- and small- scale measurement campaigns to investigate the channel characteristics in various environments [4]. The large-scale characteristics are identified by the channel's path loss exponent (PLE) and the shadow fading (SF) standard deviation [5]. On the other hand, small-scale measurements are carried out to characterize the wireless channel impulse response (CIR) or its power delay profile (PDP) [6].

In this paper, the results of a small-scale measurement campaign carried at the American University of Sharjah (AUS) campus in Sharjah, United Arab Emirates (UAE) are reported. The measurements were conducted using a 250 MHz wideband signal modulating a 24 GHz carrier. Further, the measurements were performed in various indoor environments within AUS College of Engineering (CEN) building. To the best of the authors' knowledge, no similar indoor measurement campaigns are reported in the Arabian Peninsula region. The work presents a followup to the authors' large-scale measurement campaign presented earlier in [7]. The paper is organized as follows: in Section II the measurement hardware and procedures are outlined; in Section III the measurement locations are described; and in Section IV the results are shown and discussed. Finally, the paper is concluded in Section V.

II. Measurement Setup

A. Measurement Hardware

The measurement setup used in performing the study is a wideband correlation-based channel sounder built using commercial off-the-shelf (COTS) components along with several instruments. The channel sounder is designed to have a 4 ns temporal resolution with a maximum multipath length of 1.226 μs. The measurement carrier frequency is set at 24 GHz. The block diagram of the transmitter (TX) and receiver (RX) sections are shown in Fig. 1.

In the transmitter section, Agilent's M9331A arbitrary wave generator was utilized to generate a pseudo-noise (PN) sequence with a rate of 250 Mcps, which was modulated by a 1.5 GHz intermediate frequency (IF) continuous wave (CW) signal. The generator's output was then up-converted by a mixer driven by a local oscillator (LO) tuned at 12 GHz. The mixer's output was input to a frequency doubler followed by a power amplifier, which fed a WR-28 15 dBi horn antenna with 30° beamwidth. The output power before the horn antenna was 12 dBm.

The receiver section consisted of another WR-28 horn antenna, whose output was fed to a low-noise amplifier (LNA). The amplifier's output was down-converted by a mixer driven by an LO tuned at 22.5 GHz. The mixer's output was input to Tektronix's MS05204 high-speed mixed signal oscilloscope. The data from the oscilloscope was imported to a workstation running MATLAB for further analysis.

Except for the instruments, the TX and RX components were contained within custom-designed boxes that were mounted on tripod with a 3-way head. The horn antennas of TX and RX were fixed at a height of 1.2 m above the ground.

B. Measurement Analysis

After importing the measurements into MATLAB, a cross-correlation step between the down-converted baseband received signal and the original PN sequence was performed in order to obtain the channel's PDP. The PDP was then used to obtain quantities like the average excess delay, the root-mean-square (RMS) delay spread along with the number of received resolvable multipath components.

Assuming that the PDP consists of K multipath components with the k^{th} path having an excess delay τ_k (in seconds)

978-1-7281-6535-6/20/$31.00 ©2020 IEEE

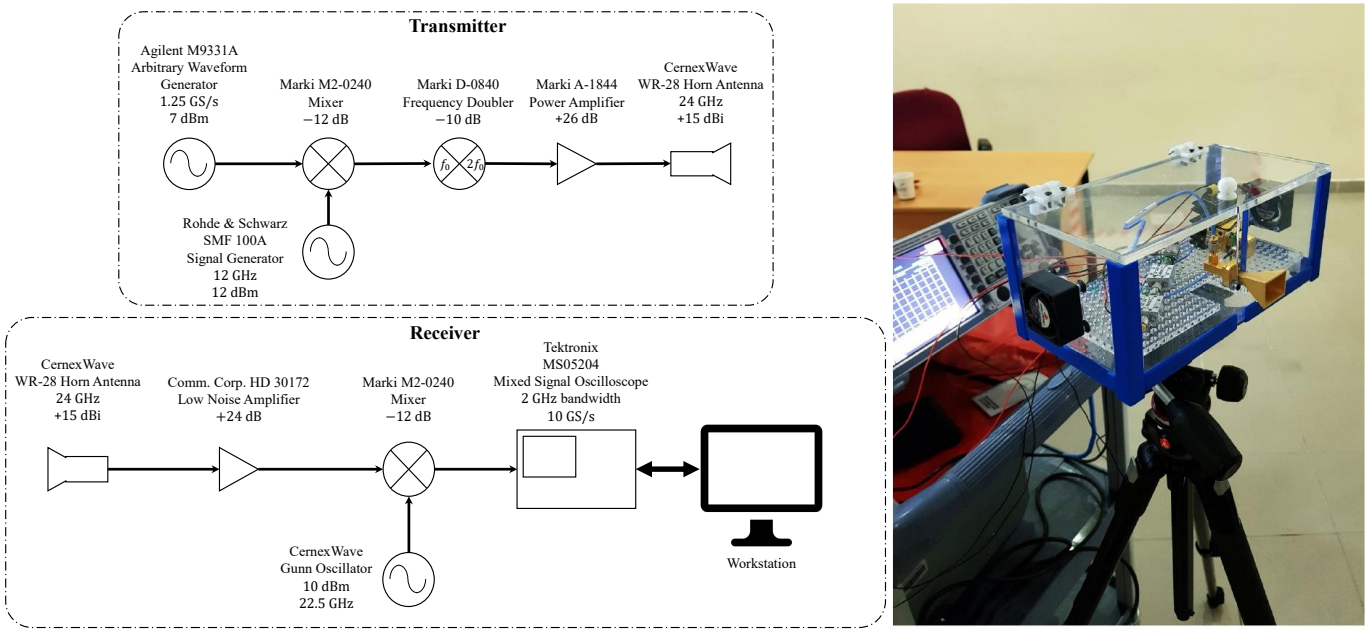

Fig. 1. Block diagram of TX and RX sections and a photo of the receiver box mounted on a tripod.

relative to the first detectable signal arriving at the receiver, the average excess delay $\overline{\tau}$ is given by

$$\overline{\tau} = \frac{\sum_{k=1}^{K} P(\tau_k)\tau_k}{\sum_{k=1}^{K} P(\tau_k)}. \quad (1)$$

Here $P(\tau_k)$ is the power of the k^{th} path (in watts). Further, the RMS delay spread (σ_τ) can be calculated as,

$$\sigma_\tau = \sqrt{\overline{\tau^2} - (\overline{\tau})^2}, \quad (2)$$

where $\overline{\tau^2}$ is the mean-square value of the excess delay given by

$$\overline{\tau^2} = \frac{\sum_{k=1}^{K} P(\tau_k)\tau_k^2}{\sum_{k=1}^{K} P(\tau_k)}. \quad (3)$$

It should be noted that resolvable paths are identified by having powers within 10 dB of the maximum detectable multipath component.

III. Measurement Scenarios

Measurements were conducted at several indoor locations in CEN building at the AUS. The locations were selected to examine the effect of various indoor environments on the small-scale characteristics of a channel. Furthermore, for each scenario, a line-of-sight (LOS) measurement was initially performed. This was followed by several measurements where the RX azimuth angle was rotated to cover 360°, with the received signal captured every 15°. A brief description for each location is discussed next.

A. Microwave Engineering Laboratory

The microwave engineering laboratory (lab) is located in the basement of CEN. It has an area of 15.7×15.7 m^2 with two long rectangular lab benches as shown in Fig. 2(a). In addition to the furniture, a small clean room as well as a small office are located within the lab. For performing measurements, the TX and RX were placed 10 m apart from each other in the middle of the laboratory as shown in the figure. The roof of the lab has a low-profile and is covered with a false ceiling.

B. Power Engineering Laboratory

The power engineering lab is a 16×20 m^2 room with a high-profile ceiling as shown in Fig. 2(b). The lab has two long rectangular benches, where large machinery and lab equipment are placed. Within the lab, there are two small offices located on the opposite corners of the room as shown in the figure. Two sets of measurements were collected in the lab with the locations of the TX and RX depicted in the figure. In the first measurement, LOS communication was established with a 7 m separation between TX and RX. For the second measurement, the separation was increased to 14 m, however due to the presence of obstacles in the lab, the LOS link was lost; thus leading to a non-LOS (NLOS) connection.

C. Corridor

Measurements were conducted in a long corridor located in the basement of the CEN building. The corridor was approximately 28 m long and 4 m wide with a height of 3 m from the floor to the ceiling. The TX was placed at one end of the corridor as shown in Fig. 2(c), with measurements conducted at two RX locations 10 m and 20 m away from the TX.

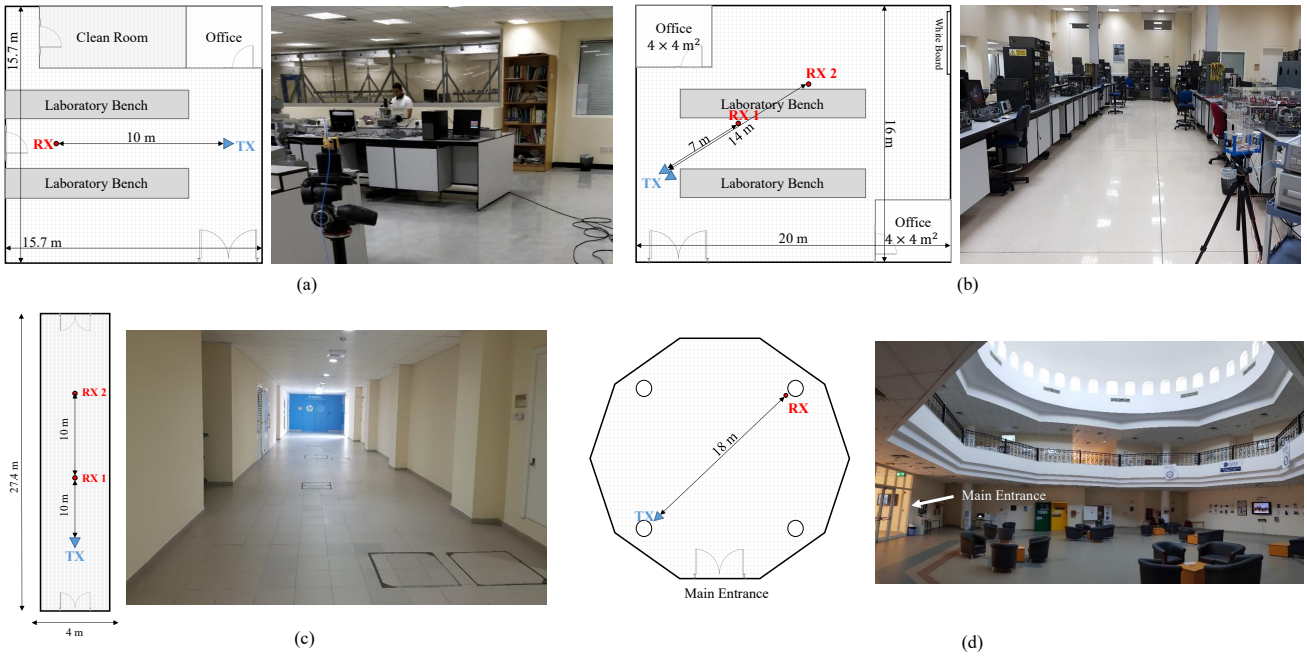

Fig. 2. Indoor measurement locations at College of Engineering at the American University of Sharjah, United Arab Emirates (not to scale): (a) microwave engineering lab, (b) power engineering lab, (c) corridor, and (d) CEN rotunda.

D. CEN Rotunda

The CEN building rotunda is characterized by its high dome-shaped ceiling as shown in Fig. 2(d). The TX and RX were positioned at opposite corners of the rotunda with an 18 m separation between them. Measurements were conducted twice: once during after-hours when the building was empty of people, and again during normal working hours with people moving around the rotunda.

IV. Results and Discussion

In this section, the results of the measurement campaign are presented in Fig. 3. For each scenario, an angle-of-arrival (AOA) measurement was obtained with the results showing a polar plot of the RX power (in dBm) versus the RX antenna steering angle with respect to the TX antenna LOS location. Such plots are useful in identifying the resulting angular spread of the signal. Moreover, the number of resolvable multipath components, the average excess delay ($\overline{\tau}$), and RMS delay spread (σ_τ) for every 30° RX azimuth angles were calculated.

In the microwave engineering lab, at most of the RX angles, the LOS component is dominant resulting in less multipath components detected (since the threshold is set to be 10 dB from the strongest path). The microwave engineering lab environment doesn't cause a lot of reflections; this is not the case for either the power engineering lab or the corridor.

In the power engineering lab there are a lot of bulky machines that can cause multiple signal reflections, which is captured by the increase in both the number of resolvable multipath components and the average excess delay. Further, in the power engineering lab, there is a clear distinction between the LOS and NLOS results. Specifically, the number of multipath components has significantly increased from 7 to 52 when the RX antenna is at 210° to the boresight. Moreover, the RMS delay spread also significantly increased from 10.3 ns to 169 ns.

As for the corridor measurements, similar to the power engineering lab results, there is an increase in the number of resolvable components and excess delay in comparison to the microwave engineering lab. This could be attributed to the multiple reflections from the side walls along the corridor path, mimicking the propagation behavior inside a waveguide.

For the fourth measurement scenario in the CEN rotunda, with the people's presence, the excess delay, RMS delay and received power decreased. This could be the result of signal blockage due to presence of people, which will limit the number of directions from which multipath components can reach the RX antenna.

V. Conclusion

Wideband small-scale measurements were conducted at 24 GHz carrier frequency with a signal bandwidth of 250 MHz. The measurements were conducted at several indoor environments that included labs, a corridor and a building rotunda. In each measurement scenario, the channel power delay profile, the angle-of-arrival (AOA) spread, the number of resolvable multipath components, the excess delay and the RMS delay spread were found. The AOA results show that the nature of an indoor environment has a significant effect on the channel characteristics. The results show the need for using adaptive antenna arrays and beamforming techniques at the TX and RX antennas to improve next generation mm-Wave 5G cellular systems performance.

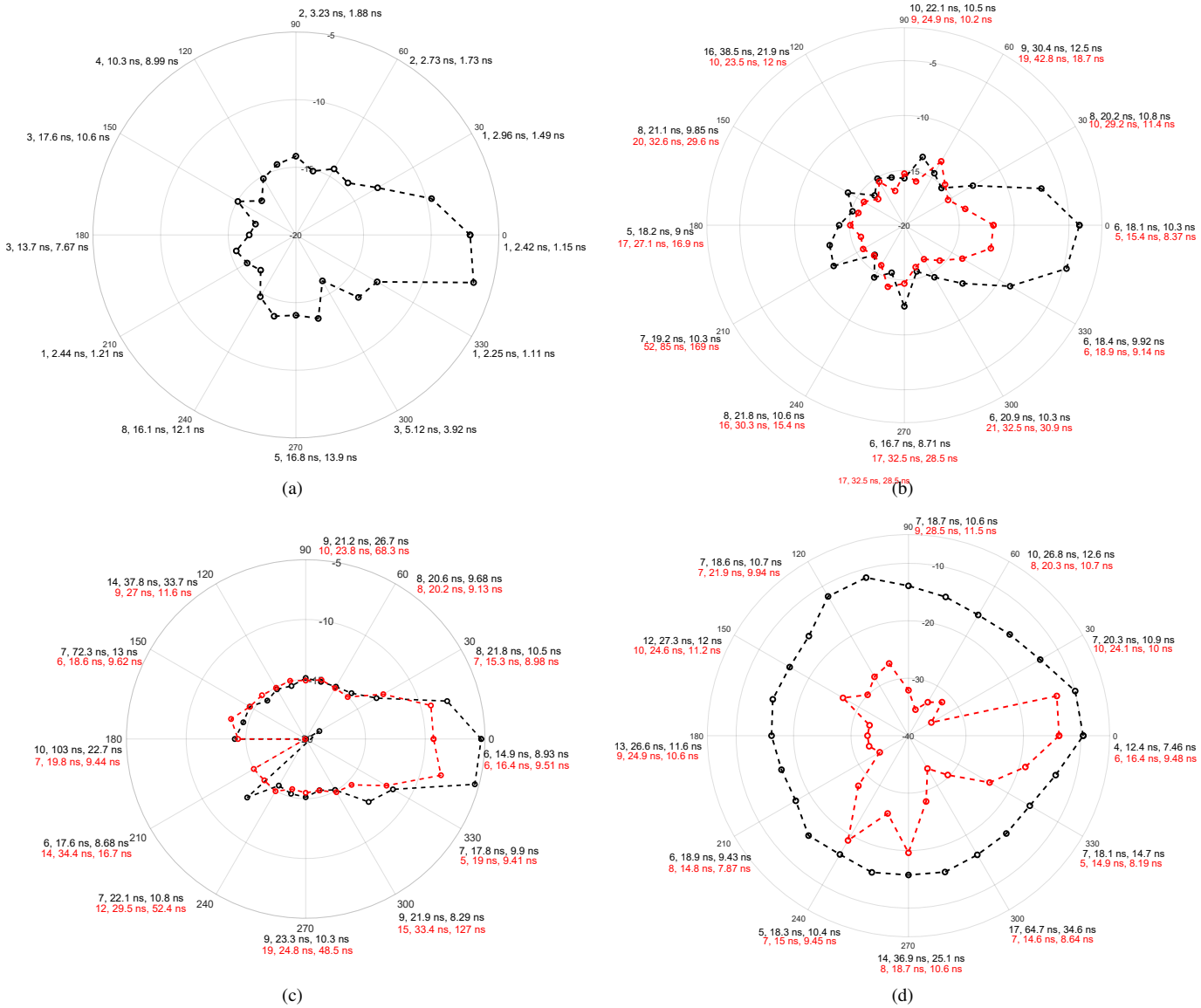

Fig. 3. AOA polar plot for the received power in dBm at the RX in different indoor scenarios (a) microwave engineering lab, (b) power engineering lab (black: LOS 7 m TX-RX separation, red: NLOS 14 m TX-RX separation), (c) corridor (black: 10 m TX-RX separation, red: 20 m TX-RX separation) and (d) CEN rotunda with 18 m TX-RX separation (black: Empty, red: crowded with people). The plot also shows the number of resolvable multipath components, the excess delay and the RMS delay spread versus the RX azimuth angle in steps of 30°.

ACKNOWLEDGMENT

This work is supported by two Faculty Research Grants (FRG16-R-25 and EFRG18-SCR-CEN-31) from the American University of Sharjah.

REFERENCES

[1] Ericsson, "Ericsson Mobility Report," February 2019. [Online]. Available: https://www.ericsson.com/assets/local/mobility-report/documents/2019/emr-q4-update-2018.pdf

[2] ——, "Internet of Things Forecast," 2019. [Online]. Available: https://www.ericsson.com/en/mobility-report/internet-of-things-forecast

[3] 3GPP, "3rd Generation Partnership Project; Technical Specification Group Services and System Aspects; Release 15 Description; Summary of Rel-15 Work Items (Release 15)," 2019.

[4] J. Huang, Y. Liu, C.-X. Wang, J. Sun, and H. Xiao, "5G Millimeter Wave Channel Sounders, Measurements, and Models: Recent Developments and Future Challenges," *IEEE Communications Magazine*, vol. 57, no. 1, pp. 138–145, 2019.

[5] T. S. Rappaport, S. Sun, R. Mayzus, H. Zhao, Y. Azar, K. Wang, G. N. Wong, J. K. Schulz, M. Samimi, and F. Gutierrez, "Millimeter Wave Mobile Communications for 5G Cellular: It Will Work!" *IEEE Access*, vol. 1, pp. 335–349, 2013.

[6] T. S. Rappaport, G. R. MacCartney, S. Sun, H. Yan, and S. Deng, "Small-scale, Local Area, and Transitional Millimeter Wave Propagation for 5G Communications," *IEEE Transactions on Antennas and Propagation*, vol. 65, no. 12, pp. 6474–6490, 2017.

[7] M. Abo Rahama, Y. Hatahet, A. Zakaria, M. H. Ismail, and M. El-Tarhuni, "Large-Scale Channel Measurements at 28 GHz in the United Arab Emirates for 5G systems," in *2019 IEEE RWS*, Jan 2019.